Genome-wide Association Study and Identifying Candidate Genes for Intramuscular Fat Fatty Acid Compositions in Ningxiang Pigs

Qinghua Zeng , Hu Gao , Shishu Yin , Yinglin Peng , Fang Yang , Yawei Fu , Xiaoxiao Deng , Yue Chen , Xiaohong Hou , Qian Wang , Zhao Jin , Gang Song , Jun He , Yulong Yin * , Kang Xu *

Posted Date: 28 July 2023

doi: 10.20944/preprints202307.2033.v1

Keywords: longissimus dorsi; saturated fatty acids; monounsaturated fatty acids; polyunsaturated fatty acid; GWAS

Article

Genome-wide Association Study and Identifying Candidate Genes for Intramuscular Fat Fatty Acid Compositions in Ningxiang Pigs

Qinghua Zeng [1,†], Hu Gao [1,3†], Shishu Yin [1], Yinglin Peng [4], Fang Yang [1], Yawei Fu [1,3], Xiaoxiao Deng [3], Yue Chen [3], Xiaohong Hou [3], Qian Wang [1,3], Zhao Jin [1,3] Gang Song [1,3], Jun He [1], Yulong Yin [1,2,3] * and Kang Xu [2,3] *

[1] College of Animal Science and Technology, Animal Nutrition Genome and Germplasm Innovation Research Center and Hunan Provincial Key Laboratory for Genetic Improvement of Domestic Animal, Hunan Agricultural University, Hunan, Changsha, China, 410128; chuweixiang168168@163.com (Q.Z.); gaohu_20190008@163.com (H.G.); yinshishu2019@126.com (S.Y.); y621829@163.com (F.Y.); fuyw2020@163.com (Y.F.); wangq0130@163.com (Q.W.); jz2725552543@163.com (Z.J.); sg19971109@163.com (G.S.); hejun@hunau.edu.cn (J.H.)

[2] Guangdong Laboratory for Lingnan Modern Agriculture, Guangzhou, China, 510642

[3] The Institute of Subtropical Agriculture, The Chinese Academy of Sciences, Laboratory of Animal Nutrition Physiology and Metabolism, Hunan, Changsha, China, 410125; 2017102040003@whu.edu.cn (X.D.); 18837025618@126.com (Y.C.); 17865669807@163.com (X.H.);

[4] Hunan Institute of Animal & Veterinary Science, Hunan, Changsha, China, 41013; 13907487646@126.com

* Correspondence: yinyulong@isa.ac.cn (Y.Y.); E-mail: xukang2020@163.com (K.X.)

Simple Summary: In this study, we conducted a comprehensive investigation of the fatty acid composition in Ningxiang pigs using a genome-wide association study. Our findings unveiled a combination of previously reported and novel candidate genes associated with saturated fatty acids (SFAs), monounsaturated fatty acids (MUFAs), and polyunsaturated fatty acids (PUFAs) in Ningxiang pigs. Notably, we identified significant SNPs that are closely linked to specific fatty acids, and some of these genes exhibited a substantial explained phenotypic variance. These noteworthy discoveries have the potential to significantly improve meat quality and fat deposition in Ningxiang pigs through targeted breeding approaches. Our research contributes valuable insights into the intricate composition of fatty acids, thus offering practical implications for elevating meat quality, and ultimately benefiting both the pig industry and consumers. The significance of this study is underscored by its potential to drive positive changes in society by promoting healthier and superior-quality pork products.

Abstract: Ningxiang pigs exhibit a diverse array of fatty acids, making them an intriguing model for exploring the genetic underpinnings of Fatty acid metabolism. In this study, we conducted a genome-wide association study using a dataset comprising 50,697 SNPs and samples from over 600 Ningxiang pigs. Our investigation yielded novel candidate genes linked to five saturated fatty acids (SFAs), four monounsaturated fatty acids (MUFAs), and five polyunsaturated fatty acids (PUFAs). Remarkably, 37, 21, and 16 SNPs showed significant associations with SFAs, MUFAs, and PUFAs, respectively. Notably, ALGA0047587, H3GA0046208, DRGA0016063, and ALGA0031262 demonstrated substantial phenotypic variance (≥ 30%) in Arachidic acid (C20:0), Elaidic Acid (C18:1n-9(t)), and Arachidonic acid (C20:4n-6), respectively. Several significant SNPs were positioned proximally to previously reported genes. In total, we identified 11, 6, and 5 candidate genes associated with SFAs, MUFAs, and PUFAs, respectively. These findings hold great promise for advancing breeding strategies aimed at optimizing meat quality and enhancing lipid metabolism within the intramuscular fat (IMF) of Ningxiang pigs.

 doi:10.20944/preprints202307.2033.v1

Keywords: *longissimus dorsi*; saturated fatty acids; monounsaturated fatty acids; polyunsaturated fatty acid; GWAS

1. Introduction

The Ningxiang pig, a renowned local pig breed in China, enjoys popularity in the market due to its exceptional flavor and taste. As an obese-type pig, research has shown that it outperforms breeds with a high lean meat rate in terms of intra-muscular fat (IMF) [1,2]. Moreover, a comparative investigation of the meat flavor between Ningxiang pigs and Duroc pigs demonstrated that the former displayed a more abundant and elevated level of volatile flavor compounds in contrast to the latter [3]. By utilizing Ningxiang pigs as the female parent in hybrid combinations, the meat quality and flavor of Duroc pigs can be effectively enhanced [4]. Consequently, owing to their exceptional germplasm traits, Ningxiang pigs have become one of the most significant breeding resources.

Pork flavor and nutritional value are closely associated with its IMF content and fatty acid composition. And fatty acid plays a critical role as fat-soluble flavor precursors in pork [5,6]. Previous studies have reported that carbonyl groups in fats undergo dehydration and cyclization, resulting in the production of meat-flavored lactone compounds. These compounds can generate flavor substances through double-bond cleavage [7]. The type and content of fatty acid, as well as the oxidation method, can influence meat flavor. Certain fatty acids have a significant impact on the formation of volatile flavor compounds. For instance, linoleic acid, linolenic acid, and arachidonic acid are positively correlated with the production of volatile flavor compounds [8,9]. Additionally, eicosapentaenoic acid (C20:5n-3, EPA) and docosahexaenoic acid (C22:6n-3, DHA) can suppress the sour and bitter taste in mutton while enhancing its fresh and sweet taste [10]. Monounsaturated fatty acids (MUFAs) can markedly affect meat color [11], particularly C18:1, which is resistant to oxidation and contributes to favorable tenderness and flavor in beef [12,13]. Moreover, the type and content of fatty acid in meat diets can impact human health. For example, linoleic acid aids in slowing down the progression of atherosclerosis [14]. Furthermore, the ratios of n-3, n-6, and other polyunsaturated fatty acids (PUFA) are closely related to human diseases such as cardiovascular disease, depression, as well as growth and development [15–17]. In summary, the fatty acid profile of pork serves as one of the crucial evaluation criteria for meat quality.

Genome-wide association studies (GWAS) can efficiently and accurately identify candidate genes related to target traits using SNPs as genetic molecular markers. In recent years, researchers have discovered numerous candidate genes associated with porcine IMF deposition and fatty acid composition through GWAS. Wang et al. [18] conducted GWAS research on the meat quality traits of 453 Lulai black pigs, identified 43 SNP loci significantly associated with IMF. These loci were annotated using the Ensembl database, resulting in the identification of 42 candidate genes related to fat deposition. Viterbo et al. [19] performed GWAS analysis on the fatty acid composition of 480 purebred Duroc pigs, identifying 25, 29, and 16 SNP loci significantly associated with stearic acid, oleic acid, and SFA, respectively. Zhang et al. [20] conducted association analysis on 33 fatty acid metabolic traits in five pig populations, identifying 865 SNPs. In addition to confirming the seven previously reported QTL regions with strong associations, they also revealed four new QTL regions. The genetic factors contributing to the fatty acid composition of Ningxiang pigs remain unknown. This study aims to examine significant candidate genes for specific fatty acid compositions and explore potential biological pathways by conducting GWAS on the fatty acid composition of Ningxiang pigs.

2. Materials and Methods

2.1. Collecting Longissimus Dorsi Samples

Longissimus dorsi samples (taken from the 6th to 12th ribs) were collected from 691 Ningxiang pigs that were slaughtered at a predetermined age (180 ± 5 days age) from the Ningxiang Chu Weixiang Slaughterhouse and Meat Processing, LLC (Hunan Province, China). A sample of

Preprints (www.preprints.org) | NOT PEER-REVIEWED | Posted: 28 July 2023 doi:10.20944/preprints202307.2033.v1

approximately 2 * 2 cubic centimeters in size was quickly taken and stored in a self-sealing bag with dry ice for IMF measurement. Additionally, the samples used for DNA extraction were simultaneously stored in a liquid nitrogen tank.

2.2. Determining Intramuscular Fat and Fatty Acids

In this study, we used the Soxhlet extraction to measure the IMF contents of 691 muscle according to the standard "Meat and Meat Products - Determination of Free Fat Content" (GB/T 9695.1-2008). The composition of fatty acids was determined by gas chromatography, with specific operations detailed below: Firstly, accurately weigh 0.5 g of sample powder dried to a constant weight and place it in a 10 mL centrifuge tube. Add 2 mL of a benzene and petroleum ether mixture (1:1 by volume), wrap it in tin foil, and let it stand in a dark place for 24 hours. Then add 2 mL of a 0.4 mol/L KOH methanol solution for methylation. Shake well and let stand for 15 minutes. Add double-distilled water to 10 mL and centrifuge at 10,000 rpm for 10 minutes to obtain 100 μL of the supernatant. A gas chromatograph (Agilent 7890A, Shimadzu, Japan) was used to determine the content of medium- to long-chain fatty acids. The GC analysis conditions were: the chromatographic column was an SP-2560 (100 m × 0.25 mm, 0.20 μm) capillary column with high-purity nitrogen as the carrier gas. The heating program was as follows: initial temperature of 140 °C, maintained for 5 minutes, increased to 240 °C at 4 °C/min; sample inlet temperature of 260 °C; FID detector temperature of 260 °C; split ratio of 100:1; and injection volume of 1 μL. A total of 25 substances were detected (Table S1), and only those presented in more than 80% of individuals (N ≥ 533) were retained (Table 1).

2.3. DNA Extraction, Genotyping and Quality Control

2.3.1. DNA Extraction, Genotyping

Genomic DNA was extracted from muscle tissue using standard phenol-chloroform method, and the DNA was dissolved in TE buffer. The concentration and purity of DNA samples were measured using the Nanodrop 2000 spectrophotometer. The samples with $A_{260/280}$ ratio between 1.7~2.0 were genotyped using the GeneSeek Genomic Profiling (GGP) version 2 Porcine 50K SNP chip (Neogen Corporation, Lincoln, NE, USA), which comprises 50,697 SNP loci.

2.3.2. Quality Control and Genotype Imputation

Firstly, SNPs located on the sex chromosome and unknown or duplicate locations were removed. To decrease the missing genotype rate, Beagle 5.1 software [21] was employed to impute the remaining 38,817 SNPs. And then, quality control was conducted using PLINK v1.9 [22] with the following criterion: (1) SNP call rate ≥ 90%; (2) minor allele frequency (MAF) ≥ 1%; (3) Hardy-Weinberg Equilibrium (HWE) testing p-value ≥ 10^{-6}. After quality control, 11,806 and 395 loci were removed due to genotype missing rate, MAF, and HWE, respectively. Finally, 691 individuals and 25,809 SNPs remained for subsequent analysis (Figure 1).

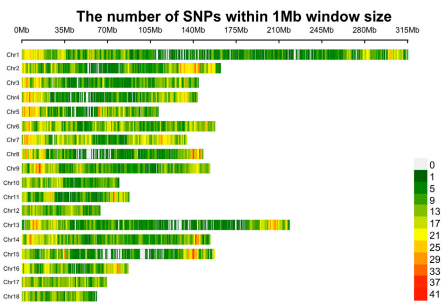

Figure 1. Distribution plot of SNPs after quality control.

Preprints (www.preprints.org) | NOT PEER-REVIEWED | Posted: 28 July 2023 doi:10.20944/preprints202307.2033.v1

2.4. Population stratification

To mitigate the risk of concealed population stratification leading to spurious results in the GWAS, we conducted principal component analysis (PCA) using imputed genotypes with PLINK v1.9 (command: --pca). As depicted in Figure 2a, the population exhibited significant population stratification, necessitating the incorporation of the first principal components (PCs) for correction.

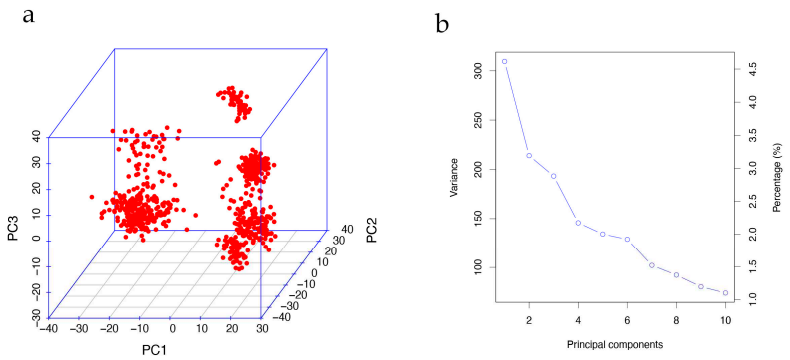

Figure 2. Principal component analysis. (a) is the visualization of the first three PC values shows the population has a population stratification; (b) is screen plot of the first 10 PC values, and decreasing trends indicate the first five PCs are appropriate to correct the population stratification.

2.5. Genome-wide association study

The association between SNPs and fatty acids was examined using the BLINK model (Bayesian-information and Linkage-disequilibrium Iteratively Nested Keyway) by GAPIT 3.0 package [23]. BLINK, an enhanced version of FarmCPU, enhances statistical power by relaxing the assumption of even distribution of trait-related genes across the genome, and incorporates Bayesian information content (BIC) in fixed-effect models to improve computational efficiency [24]. The model integrates equations (1), (2), and (3) based on the BIC strategy, iteratively calculating and excluding all pseudo quantitative trait nucleotides (QTNs) to identify significant loci.

$$y = Xa + Zb + e \qquad (1)$$

$$y = Xa + Zb + Qp + e \qquad (2)$$

$$y = Xa + Qp + e \qquad (3)$$

Where y is a vector of phenotypic data, a is the vector of fixed effect, including IMF content and the first five PCs; b is a vector of marker effect; and p is the effect of pseudo QTNs. X, Z, and Q are the incidence matrices correspoding to a, b, and p, respectively. And e is the vector of residual errors. The BLINK model use equation (1) to define pseudo QTNs as a covariate for equation (2). The SNP obtained from equation (2) determines the information of QTNs based on LD, and then employs equation (3) to perform accuracy detection of QTNs using the BIC strategy. The false discovery rate (FDR) method of multiple testing, as described by Benjamini-Hochberg, was utilized to measure the statistical significance of association studies at a genome-wide level. The cut-off threshold for considering SNPs as significant was set at FDR ≤ 0.1. The explained phenotypic variance (PVE) was calculated as follows [25]:

$$PVE = \frac{2\alpha^2 MAF(1-MAF)}{2\alpha^2 MAF(1-MAF)+(se(\alpha^2)2N\times MAF(1-MAF)} \qquad (4)$$

Where MAF is the minior allele frequency for SNP, α^2 is the effect of SNP marker, and N is the sample size. $se(\alpha^2)$ is the standard error of α^2.

Preprints (www.preprints.org) | NOT PEER-REVIEWED | Posted: 28 July 2023 doi:10.20944/preprints202307.2033.v1

2.6. Estimation of Hertability and Genetic correlation

The hertability (h^2) calculated by following formula (5) which completed by HIBLUP [26]:

$$h^2 = \frac{\sigma_a^2}{\sigma_a^2+\sigma_e^2} \qquad (5)$$

Where σ_a^2 and σ_e^2 are the additive genetic variance and the residual variance, respectively. The phenotypic and genetic correlation (r_p and r_g) between IMF and FAs were estimated using HIBLUP software [26].

$$r_P = \frac{COV_{P_{xy}}}{\sqrt{\sigma_{P_x}^2 \times \sigma_{P_y}^2}};\ r_G = \frac{COV_{G_{xy}}}{\sqrt{\sigma_{G_x}^2 \times \sigma_{G_y}^2}} \qquad (6)$$

Where $COV_{P_{xy}}$ and $COV_{G_{xy}}$ represent the phenotypic and genetic covariance, respectively. σ_P^2 and σ_G^2 are the phenotypic and genetic vanriance, respectively.

2.7. Identificaiton of Candidate Genes

Candidate genes were identified according to their physical positions and functions based on the Sus scrofa 10.2 reference genome assembly. The SNP-containing or nearest annotated genes for each potential SNP were obtained from Sus scrofa (10.2) gtf file (http://ftp.ensembl.org/pub/release-80/gtf/sus_scrofa/Sus_scrofa.Sscrofa10.2.80.gtf.gz) and taken as candidate genes.

2.8. Functional Enrichment analysis

The g:profier website [27] was used to Gene Ontology (GO) and Kyoto Encyclopedia of Genes and Genomes (KEGG) enrichment analysis. Choosing Tailor-made algorithm for multiple testing correstion (adjust p value < 0.05).

3. Results

3.1. Descriptions Statistics of IMF and fatty acids composition

The statistical analysis results of IMF and 25 fatty acids are presented in Table S1. The IMF content in the *longissimus dorsi* of Ningxiang pigs was determined to be 3.65%. The overall fatty acid distribution revealed the highest proportion of MUFA at 41.88%, followed by SFA at 39.35%, and the lowest was PUFA (12.78%). Eleven fatty acids were removed due to a sample size below 553 individuals (< 80%), such as C22:6n-3, C17:1, and C15:0. And the remaining 14 fatty acids, IMF were used to following analysis (Table 1). Among these fatty acids, Oleic acid (C18:1n-9(c)) exhibited the highest content (40.28%), while Elaidic Acid (C18:1n-9(t)) had the lowest content (0.11%).

Table 1. Detailed information on 25 fatty acids present in IMF of the longissimus dorsi of Ningxiang pigs.

Fatty acid	N	Relative Content (± Sd) (%)	h^2 (± Sd)
IMF (Intramuscular Fat)	691	3.65 (± 1.00)	0.72 (± 0.02)
SFA (Saturated fatty acid)	**691**	**39.35 (± 10.01)**	**0.61 (± 0.04)**
C14:0 (Myristic acid)	649	1.42 (± 0.24)	0.80 (± 0.03)
C16:0 (Palmitic acid)	651	26.38 (± 1.46)	0.76 (± 0.03)
C17:0 (Margaric acid)	645	0.15 (± 0.03)	0.45 (± 0.08)
C18:0	651	13.42 (± 1.62)	0.89 (± 0.02)

 doi:10.20944/preprints202307.2033.v1

(Stearic acid)			
C20:0 (Arachidic acid)	649	0.21 (± 0.05)	0.87 (± 0.04)
MUFA (Monounsaturated fat acid)	**691**	**41.88 (± 10.92)**	**0.84 (± 0.02)**
C16:1 (Palmitoleic Acid)	650	3.28 (± 1.03)	0.87 (± 0.03)
C18:1n-9(t) (Elaidic Acid)	627	0.11 (± 0.03)	0.37 (± 0.09)
C18:1n-9(c) (Oleic acid)	651	40.28 (± 3.13)	0.74 (± 0.03)
C20:1 (Eicosenoic acid)	650	0.80 (± 0.29)	0.78 (± 0.03)
PUFA (Polyunsaturated fatty acid)	**691**	**12.78 (± 4.80)**	**0.60 (± 0.03)**
C18:2n-6(c) (Linoleic acid)	651	10.12 (± 2.57)	0.61 (± 0.03)
C18:3n-3 (α-Linolenic acid: ALA)	572	0.36 (± 0.19)	0.63 (± 0.08)
C20:2 (Eicosa-11,14-dienoic acid)	649	0.33 (± 0.08)	0.67 (± 0.05)
C20:3n-6 (Dihomo-γ-linolenic acid)	647	0.38 (± 0.14)	0.88 (± 0.03)
C20:4n-6 (Arachidonic acid)	649	2.42 (± 1.00)	0.55 (± 0.05)

N represents the number of individuals with this fatty acid detected in the sample population; relative content represents the mean value of the content, and Sd represents standard deviation; h^2: heritability.

3.2. Estimation of Genetic parameter

The results of the correlation analysis between fatty acids and IMF are presented in Figure 3a, b. In phenotypic correlation analysis, the majority of fatty acids exhibited a significantly correlation with IMF ($p < 0.001$), except SFA, C20:0, and C18:3n-3 ($p > 0.05$). SFA demonstrated significantly positive correlated with MUFA and PUFA ($p < 0.001$) but showed negative correlations with four MUFAs and five PUFAs ($p < 0.05$). Furthermore, SFA, MUFA, and PUFA were significantly positively correlated with five SFAs, four MUFAs, and five PUFAs, respectively ($p < 0.05$). Regarding the genetic correlation analysis, C16:1 had the highest correlation with IMF (r_g = 0.64), SFA was negatively correlated with most MUFAs and PUFAs, expect C16:1 and C18:1n-9(t). All fatty acids belonged to moderate to high heritability (0.37 ~ 0.89), of these fatty acids, C17:0 and C18:1n-9(t) demonstrated relatively low heritability estimates at 0.45 and 0.37, respectively, while most other fatty acids exhibited heritability estimates above 0.6. Notably, C18:0 exhibited the highest heritability estimate of 0.89 (Table 1).

Preprints (www.preprints.org) | NOT PEER-REVIEWED | Posted: 28 July 2023 doi:10.20944/preprints202307.2033.v1

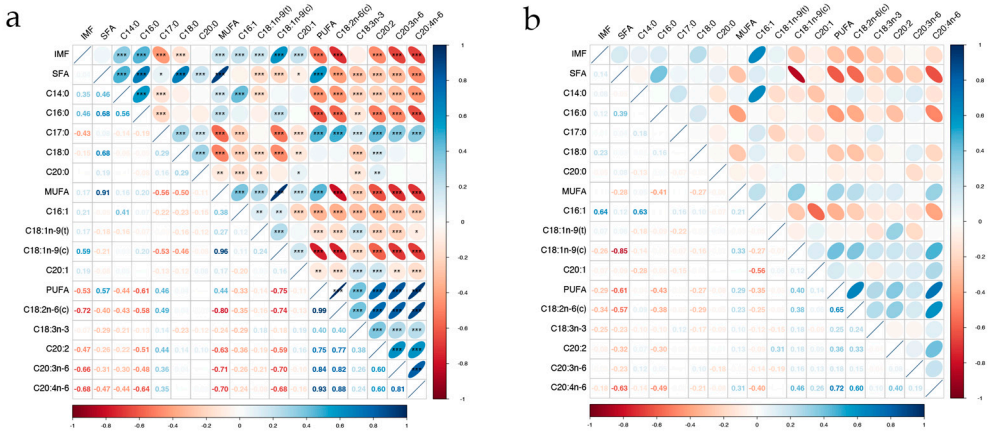

Figure 3. Correlations among IMF and 14 fatty acids in *longissimus dorsi* of Ningxiang pigs. "***" represents *p*-value < 0.001, "**" represents *p*-value < 0.01, "*" represents *p*-value < 0.05. (a) is the phenotypic correlation; (b) is the genetic correlation.

3.3. Genome-wide assciation study results for fatty acids

After quality control, 25,809 SNPs for 691 Ningxiang pigs were retained for GWAS. In total, 74 genome-wide level SNPs were identified for 14 FAs in this study.

3.3.1. SFA

In this study, 37 genome-wide level significant SNPs were identified for 5 SFAs (C14:0, C16:0, C17:0, C18:0, and C20:0), C20:0 had the most loci, which were located on SSC2, SSC3, SSC4, SSC5, SSC7, SSC8, SSC13, SSC14, and SSC16, respectively (Figure 4a to 4e). Moreove, some loci were with large explained phenopic variance, such as ALGA0047587 (89.85%), ASGA0059505 (11.39%), and DRGA0011206 (6.85%) (Table 1).

Preprints (www.preprints.org) | NOT PEER-REVIEWED | Posted: 28 July 2023 doi:10.20944/preprints202307.2033.v1

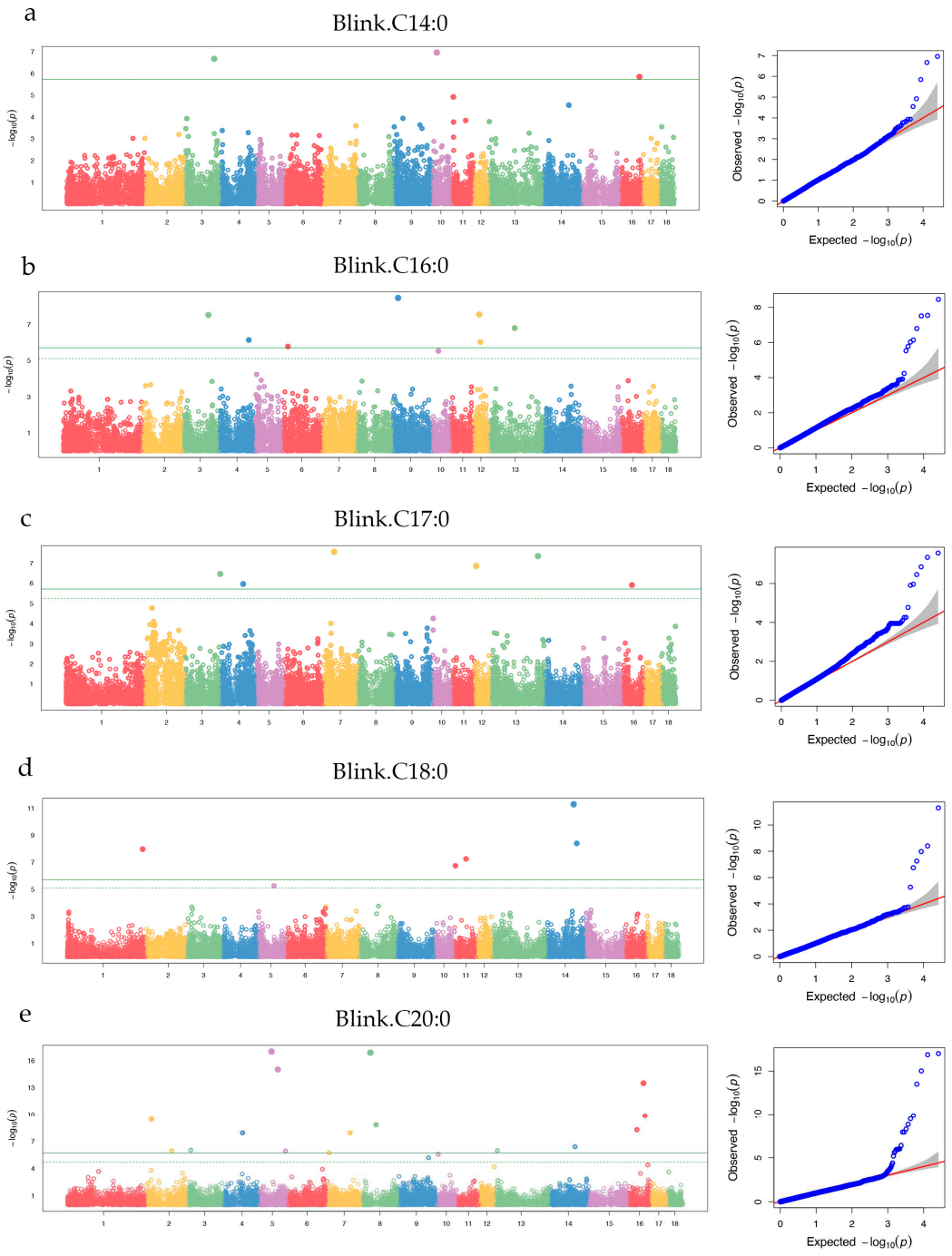

Figure 4. Manhattan plot for five SFAs (C14:0, C16:0, C17:0, C18:0, and C20:0). The x-axis represents the chromosomes, and y-axis represnts the -log10 (p_value). The green line is genome-wide level threshold, the green dashed line is chromosome-level threshold.

3.3.2. MUFA

The Manhattan plots showed 21 genome-wide level significant loci were identified on 12 chromosomes (SSC1, SSC2, SSC3, SSC4, SSC5, SSC7, SSC9, SSC11, SSC13, SSC14, SSC16, and SSC17) for four MUFAs (Figure 5a to 5d). H3GA0046208 explained the largeset phenopic variance (45.24%) for C18:1n-9(t) (Table 1).

Preprints (www.preprints.org) | NOT PEER-REVIEWED | Posted: 28 July 2023 doi:10.20944/preprints202307.2033.v1

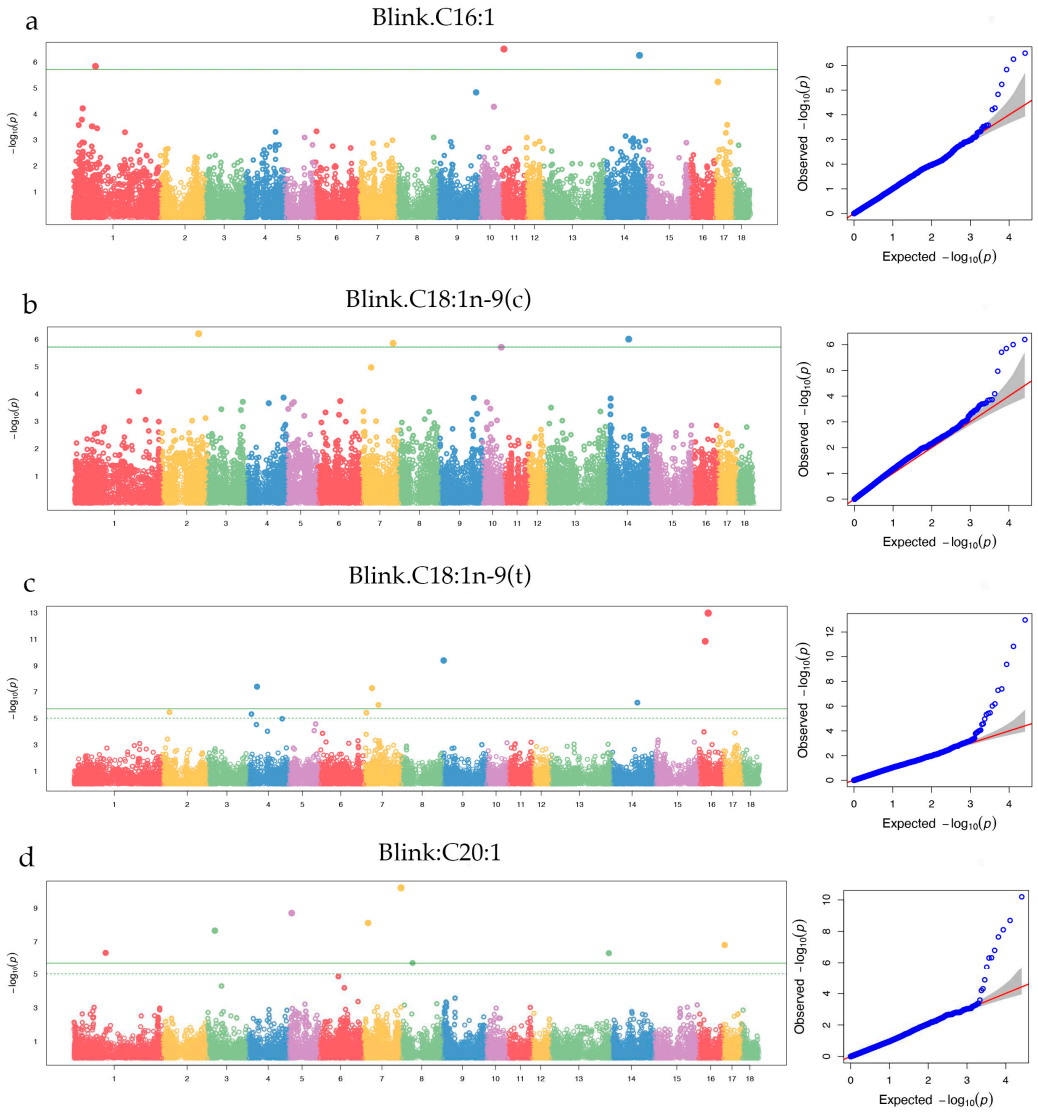

Figure 5. Manhattan plot for four MUFAs (C16:1, C18:1n-9(c), C18:1n-9(t), and C20:1). The x-axis represents the chromosomes, and y-axis represnts the -log10 (p_value). The green line is genome-wide level threshold, the green dashed line is chromosome-level threshold.

3.3.3. PUFA

The Manhattan plots showed that 16 genome-wide level significant loci on 7 chromosomes (SSC1, SSC2, SSC5, SSC8, SSC9, SSC13, and SSC16) were identified for five PUFAs (Figure 6a to 6e).

Preprints (www.preprints.org) | NOT PEER-REVIEWED | Posted: 28 July 2023 doi:10.20944/preprints202307.2033.v1

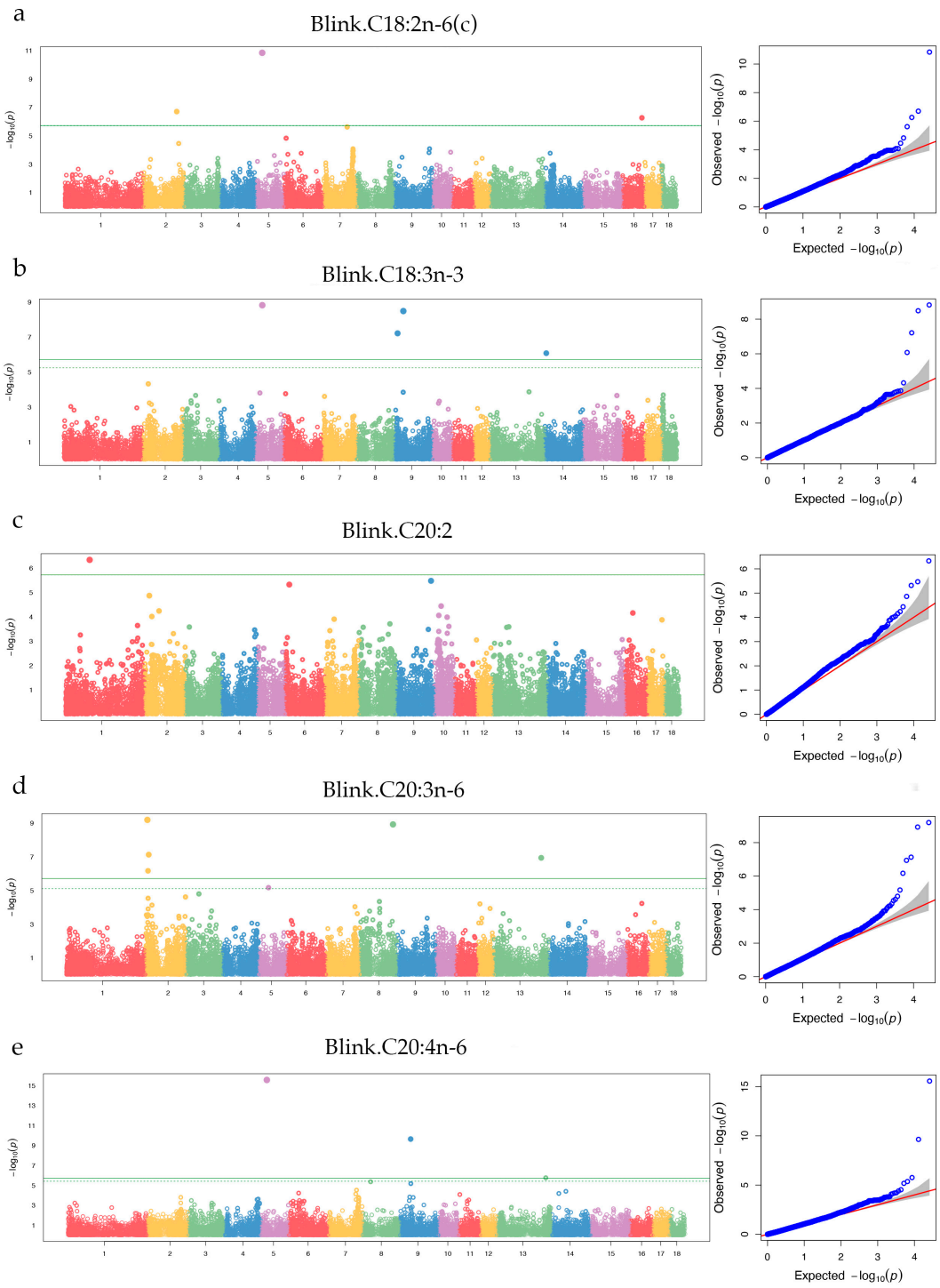

Figure 6. Manhattan plot for five PUFAs (C18:2n-6(c), C18:3n-3, C20:2, C20:3n-6, and C20:4n-6). The x-axis represents the chromosomes, and y-axis represnts the -log10 (p_value). The green line is genome-wide level threshold, the green dashed line is chromosome-level threshold.

3.4. Identification of candidate genes

Four hundred and fifty-three genes were identified within a 500 kb region upstream and downstream of the significant SNPs. For SFAs, there were 354 genes were found in 1 Mb genomic regions, and 40 genes close to 37 loci, of which 11 (WU_10.2_3_116903421, ASGA0074106, WU_10.2_4_119395133, M1GA0024654, WU_10.2_3_142168876, ALGA0010606, WU_10.2_11_3591593, ALGA0080940, H3GA0041501, MARC0054269, and WU_10.2_16_59778879) were located within 11 genes (ALK, MFAP3, CEPT1, NPEPPS, ENSSSCG00000008655, SWI5, CDK8,

Preprints (www.preprints.org) | NOT PEER-REVIEWED | Posted: 28 July 2023 doi:10.20944/preprints202307.2033.v1

AVPI1, ALOX5, ITGA1, and SLIT3), respectively. For MUFAs, 6 SNPs (ALGA0015731, ASGA0064960, H3GA0025990, H3GA0046208, WU_10.2_5_13180559, and ASGA0031521) were the intragenic variants. As for PUFAs, 19 genes were identified in 16 SNP loci.

Table 2. Genome-wide significant SNPs loci for SFAs, MUFAs and PUFAs in Ningxiang pigs.

Fatty acid	SNP	CHR	POS (bp)	MAF [1]	*p*-value	PVE (%) [2]	Candidate gene [3]	Location (bp) [4]
				SFA				
C14:0	WU_10.2_3_116903421	3	116,903,421	0.10	2.15×10^{-7}	2.98	*ALK*	Within
	H3GA0053711	10	19,975,279	0.39	1.10×10^{-7}	4.21	*HNRNPU*	(-) 46,502
	ASGA0074106	16	75,024,639	0.20	1.43×10^{-6}	6.30	*MFAP3*	Within
	ALGA0020228	3	102,155,060	0.27	3.04×10^{-8}	0.96	*CAMKMT*	(-) 67,527
	WU_10.2_4_119395133	4	119,395,133	0.20	7.24×10^{-7}	0.71	*CEPT1*	Within
C16:0	ASGA0027821	6	20,665,813	0.08	1.66×10^{-6}	1.87	---	---
	MARC0001638	9	20,050,249	0.38	3.49×10^{-9}	1.54	---	---
	M1GA0024654	12	23,711,351	0.25	2.83×10^{-8}	1.49	*NPEPPS*	Within
	ASGA0053936	12	28,196,313	0.10	9.35×10^{-7}	2.46	*CA10*	(-) 73,699
	ALGA0071522	13	101,058,816	0.48	1.60×10^{-7}	0.92	*P2RY1* / *RAP2B*	(+) 24,652 / (-) 272,878
	WU_10.2_3_142168876	3	142,168,876	0.22	3.47×10^{-7}	1.63	*ENSSSCG00000008655*	Within
	WU_10.2_4_89693248	4	89,693,248	0.13	1.09×10^{-6}	0.98	*ATP1B1* / *DPT*	(-) 142,688 / (+) 276,076
C17:0	ALGA0040777	7	41,624,144	0.44	2.75×10^{-8}	1.06	*ENSSSCG00000027922*	(-) 6,957
	WU_10.2_12_7644839	12	7,644,839	0.02	1.40×10^{-7}	5.94	*SDK2*	(-) 101,272
	ASGA0059505	13	191,280,771	0.01	4.53×10^{-8}	11.39	*ENSSSCG00000012009*	(+) 96,319
	ASGA0097154	16	38,383,883	0.35	1.23×10^{-6}	0.74	*MIER3* / GPBP1	(-) 92,572 / (+) 147,193
	ALGA0010606	1	302,716,687	0.02	1.05×10^{-8}	5.30	*SWI5*	Within
	WU_10.2_11_3591593	11	3,591,593	0.45	1.78×10^{-7}	0.96	*CDK8*	Within
C18:0	DRGA0011206	11	45,910,375	0.02	5.51×10^{-8}	6.85	*KLHL1*	(-) 344,156
	WU_10.2_14_106229446	14	106,229,446	0.09	5.06×10^{-12}	6.06	*DKK1* / *PRKG1*	(+) 111,773 / (-) 24,033
	ALGA0080940	14	118,552,421	0.30	3.94×10^{-9}	1.79	*AVPI1*	Within

Preprints (www.preprints.org) | NOT PEER-REVIEWED | Posted: 28 July 2023 doi:10.20944/preprints202307.2033.v1

	WU_10.2_2_19459316	2	19,459,316	0.01	3.53×10^{-10}	0.50	*U5 / EXT2*	(+) 53,530 / (-) 248,965
	MARC0046666	2	99,366,616	0.10	1.11×10^{-6}	0.04	*MEF2C*	(+) 481,344
	WU_10.2_3_13474115	3	13,474,115	0.17	9.65×10^{-7}	0.03	*SNORA79*	(-) 6,713
	ALGA0025658	4	75,387,791	0.03	1.21×10^{-8}	2.18	*ARMC1*	(+) 213,167
	DRGA0005776	5	46,748,561	0.01	9.76×10^{-18}	0	*IPO8*	(-) 37,690
	H3GA0016783	5	71,996,403	0.36	9.65×10^{-16}	0.12	*IL17RA / CECR2*	(+) 216,815 / (-) 1,304
	WU_10.2_5_102656712	5	102,656,712	0.01	1.17×10^{-6}	0.19	---	---
C20:0	WU_10.2_7_6641603	7	6,641,603	0.06	1.79×10^{-6}	0.04	*OFCC1*	(+) 394,140
	MARC0077077	7	90,165,851	0.03	1.22×10^{-8}	0.02	*U4*	(-) 483,532
	ALGA0047587	8	36,220,598	0.01	1.33×10^{-17}	89.85	---	---
	ALGA0049475	8	58,905,523	0.02	1.57×10^{-9}	0.38	*TMEM165 / REST*	(+) 136,496 / (-) 65,988
	WU_10.2_13_7954310	13	7,954,310	0.02	1.07×10^{-6}	0.13	*EFHB / PP2D1*	(+) 156,176 / (-) 17,027
	H3GA0041501	14	98,921,568	0.37	4.07×10^{-7}	0.02	*ALOX5*	Within
	MARC0054269	16	33,826,642	0.45	5.43×10^{-9}	0.04	*ITGA1*	Within
	WU_10.2_16_59778879	16	59,778,879	0.12	3.17×10^{-14}	0.48	*SLIT3*	Within
	ASGA0073724	16	65,860,356	0.38	1.45×10^{-10}	0.06	---	---
				MUFA				
	ALGA0004246	1	80,989,471	0.19	1.47×10^{-6}	8.55	*PREP*	(+) 97,088
C16:1	MARC0099145	11	7,302,533	0.26	3.19×10^{-7}	2.20	*ALOX5AP / MEDAG*	(+) 14,970 / (-) 94,001
	ALGA0081341	14	127,218,925	0.42	5.58×10^{-7}	2.81	*U6*	(+) 142,743
	ALGA0015731	2	132,199,278	0.37	6.33×10^{-7}	0.67	*PRDM6*	Within
C18:1n-9(c)	WU_10.2_7_113985448	7	113,985,448	0.337	1.41×10^{-6}	1.67	*FLRT2*	(-) 371,757
	ASGA0064960	14	77,566,009	0.34	9.97×10^{-7}	0.41	*RUFY2*	Within
	H3GA0012422	4	31,763,547	0.02	4.00×10^{-8}	0.73	*RSPO2*	(-) 39,304
C18:1n-9(t)	DIAS0004691	7	29,798,220	0.02	5.20×10^{-8}	1.37	*RXRB / COL11A2*	(+) 30,602 / (-) 98
	ASGA0033619	7	52,577,418	0.02	9.68×10^{-7}	0.52	*MCM3 / PAQR8*	(+) 22,826 / (-) 58,073

Preprints (www.preprints.org) | NOT PEER-REVIEWED | Posted: 28 July 2023 doi:10.20944/preprints202307.2033.v1

	H3GA0025990	9	2,779,787	0.01	4.13×10^{-10}	2.69	*SYT9*	Within
	ALGA0079386	14	91,261,955	0.29	6.50×10^{-7}	0.26	*NRG3* / *SNORA31*	(+) 153,379 / (-) 56,774
	H3GA0046208	16	22,351,887	0.01	1.46×10^{-11}	45.24	*CAPSL*	Within
	DRGA0016063	16	32,872,449	0.04	1.06×10^{-13}	31.52	*ISL1*	(+) 313,447
	ASGA0004095	1	113,473,890	0.24	4.76×10^{-7}	0.79	*ENSSSCG00000004527*	(-) 459,563
	ASGA0085560	3	26,316,304	0.36	2.27×10^{-8}	1.43	*GP2* /*GPR139*	(+) 23,724 / (-)218,640
	WU_10.2_5_13180559	5	13,180,559	0.38	2.03×10^{-9}	0.85	*CRY1*	Within
C20:1	ASGA0031521	7	17,152,543	0.02	7.91×10^{-9}	6.73	*CDKAL1*	Within
	7_134762912	7	134,762,912	0.26	6.37×10^{-11}	1.67	*SCARNA6*	(+) 112,451
	ALGA0111031	8	41,395,488	0.25	1.91×10^{-6}	2.27	*USP46*	(-) 246,632
	ASGA0059943	13	210,282,758	0.10	4.97×10^{-7}	0.82	*CLDN14* / *SIM2*	(+) 125,384 / (-) 157,224
	H3GA0047778	17	7,610,059	0.03	1.62×10^{-7}	3.49	---	---
			PUFA					
	ALGA0015731	2	132,199,278	0.37	1.99×10^{-7}	2.10	*CEP120*	Within
C18:2n-6(c)	WU_10.2_5_24153921	5	24,153,921	0.02	1.45×10^{-11}	18.22	*RDH16* / *NDUFA4L2*	(+) 14,897 / (-) 8,844
	ASGA0085192	16	76,899,854	0.05	5.47×10^{-7}	6.33	*ENSSSCG00000017077*	(+) 100,159
	MARC0014875	5	26,784,432	0.01	1.52×10^{-9}	21.92	*SLC16A7*	Within
C18:3n-3	ALGA0111381	9	14,991,770	0.02	6.15×10^{-8}	5.51	*ssc-mir-708*	(-) 128,707
	DRGA0009320	9	37,972,729	0.08	3.28×10^{-9}	16.44	*ENSSSCG00000014993*	Within
	ASGA0060681	14	5,504,363	0.42	8.41×10^{-7}	1.53	*SNORA25*	(+) 236,965
C20:2	ALGA0004743	1	96,303,394	0.08	4.70×10^{-7}	10.78	*ENSSSCG00000022379*	(-) 50,039
	WU_10.2_2_7173969	2	7,173,969	0.23	6.35×10^{-10}	2.14	*FLRT1* / *OTUB1*	(+) 76,045 / (-) 30,744
C20:3n-6	WU_10.2_2_9630034	2	9,630,034	0.19	6.76×10^{-7}	2.15	*SDHAF2*	Within
	ALGA0106081	2	12,459,648	0.18	7.40×10^{-8}	1.62	*ENSSSCG00000022943*	(+) 6,189
	ASGA0039809	8	130,628,617	0.18	1.18×10^{-9}	1.84	*EIF4E*	Within

 doi:10.20944/preprints202307.2033.v1

	ALGA0115480	13	187,857,350	0.11	1.14×10^{-7}	1.57	*ROBO2*	(+) 5,756
	ALGA0031262	5	23,686,043	0.01	2.71×10^{-16}	31.76	*PTGES3*	Within
C20:4n-6	WU_10.2_9_42529952	9	42,529,952	0.02	2.28×10^{-10}	7.56	*C11orf87* / *U1*	(+) 440,896 / (-) 52,775
	WU_10.2_13_194176619	13	194,176,619	0.22	1.73×10^{-6}	1.20	*U6*	(+) 137,764

[1] MAF: minor allelic frequency; [2] PVE: explained phenotype variance; [3] Genes name include official symbol name and ENSEMBL_ID; [4] (-) / (+) represent the significant loci located upstream / downstream of the nearest gene.

3.5. Functional Enrichment of Candidata Genes

The GO and KEGG enrichment analysis was performed using g:profier website for all fatty acids traits. The functional genes were significant enriched in 262 GO terms ($p\_adj < 0.05$) (see Appendix Materials). The top 10 molecular function were binding and so on. And the top 10 cellular component were cellular anatomical entity (GO:0110165), membrane-bounded organelle (GO:0043227) and so on. There were some GO terms associated with lipid and fatty acid metabolism in biological process (Figure 7a), such as fatty acid biosynthetic process (GO:0006633), unsaturated fatty acid metabolic process(GO:0033559), lipid biosynthetic process (GO:0008610), and lipid metabolic process (GO:0006629). In this study, annoted genes were significantly enriched in 12 KEGG pathways, such as Metabolic pathways (KEGG:01100), Inflammatory bowel disease (KEGG:05321), and Th17 cell differentiation (KEGG:04659) (Figure 7b). These KEGG pathways can be categorized into three groups on the KEGG website: Metabolism, Organismal Systems, and Human Diseases (https://www.kegg.jp/kegg/pathway.html).

Preprints (www.preprints.org) | NOT PEER-REVIEWED | Posted: 28 July 2023 doi:10.20944/preprints202307.2033.v1

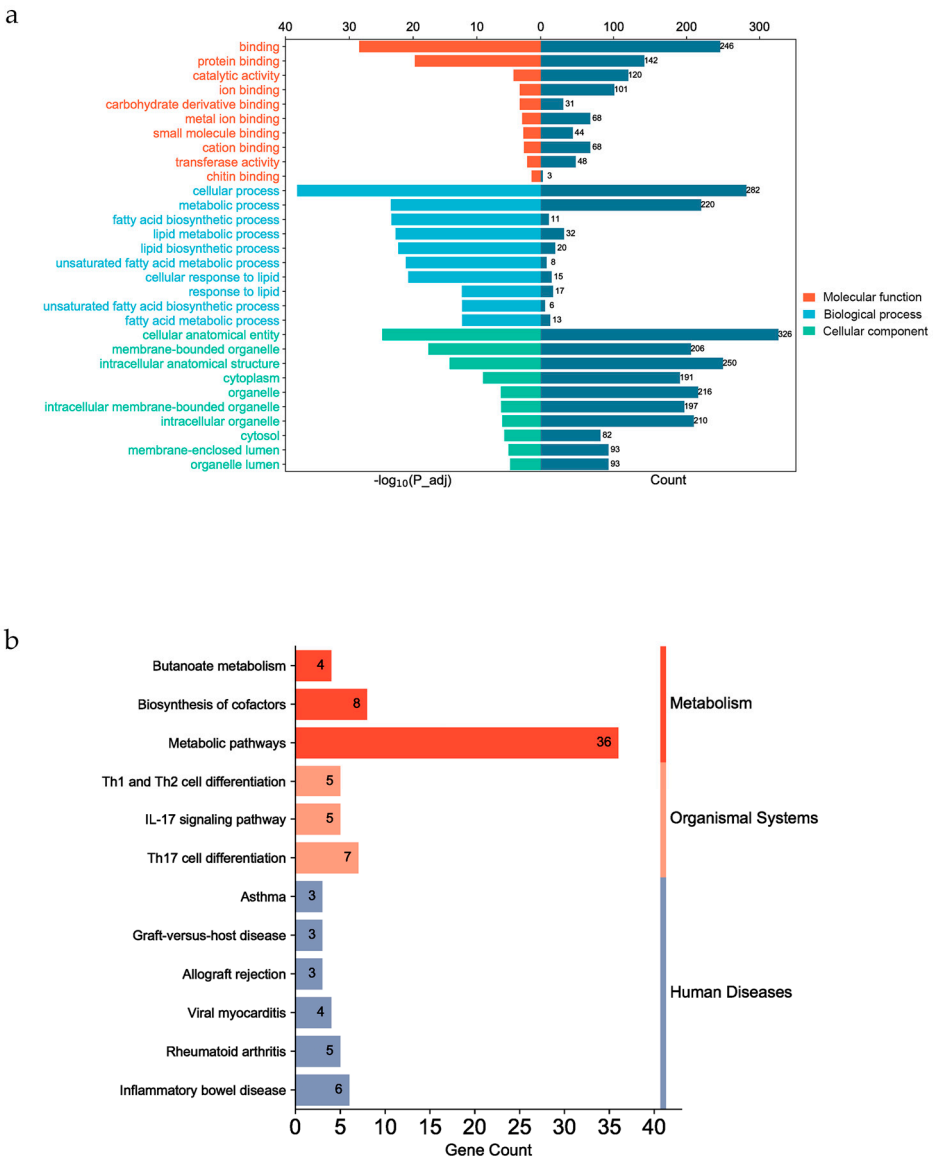

Figure 7. Gene functional enrichment analysis. (a) shows the top 10 enrichment in molecular function and cellular component and 10 bological processes associated with fatty acid and lipid metabolism. (b) shows the result of 12 KEGG enrichment, which can be divided into three categories on the kegg website (Metabolism, Organismal Systems, and Human Diseases).

4. Discussion

4.1. Phenotypic and genetic Correlations

In this study, a total of 25 fatty acids species were detected in the longissimus dorsi of Ningxiang pigs, with 14 species commonly found in the population. The SFA is the most abundant among them, while the MUFA relative content is the highest. According to research, the distribution pattern of fatty acid in various varieties of pork is quite similar. However, Jiang et al. [30] analyzed the fatty acid composition in three types of adipose tissues (dorsal subcutaneous adipose tissue, abdominal subcutaneous adipose tissue, and perirenal adipose tissue), revealing significant differences in the fatty acid profiles among the three adipose tissue types, which were also influenced by gender. Interestingly, DHA was not found in the longissimus dorsi and backfat of various pig populations, including Chinese regional and foreign pig breeds [31,32]. Nevertheless, in other studies examining the fatty acid profile of Ningxiang pigs, DHA was detected in different tissues of Ningxiang pigs

 doi:10.20944/preprints202307.2033.v1

[30,33,34]. DHA, belonging to the Omega-3 family alongside ALA and EPA [35], is a crucial PUFA for human health. It is directly associated with brain development, physical well-being, and is an essential nutrient integral to human life [36]. It is expected that among the longissimus dorsi of Ningxiang pig, both Linoleic acid ($h^2 = 0.88$) and Eicosa-11,14-dienoic acid ($h^2 = 0.63$) from the Omega-3 family exhibit high heritability, which is a rare phenomenon [37,38]. Further research has revealed that the dietary n-6/n-3 ratio can significantly impact the overall health of consumers [39]. To ensure the safety and health of pork products, pig industry breeders and researchers have long sought to enhance the PUFA content and distribution in pork [40–43]. Simultaneously, studies have found that the main characteristic aroma of Ningxiang pork is derived from alcohols, aldehydes, and ketones, with the abundance of flavor substances significantly higher than that of lean pork breeds [3]. Fatty acids, as the primary substrate of lipid oxidation, could be the reason for the characteristic aroma of Ningxiang pork.

As an important indicator pork quality, the IMF has consistently garnered significant attention. Numerous studies have also provided evidence for the impact of IMF on meat quality [44,45]. In recent years, the hypothesis that IMF deposition in muscle is impacted by fatty acid structure was verified [19,46–48]. By conducting correlation analysis between IMF and various fatty acid components in the longissimus dorsi of Ningxiang pigs (Figure 3), it was observed that IMF exhibits a notably low correlation with SFA. Furthermore, IMF exhibited a significant positive correlation with MUFA and a significant negative correlation with polyunsaturated PUFA. Particularly, a high genetic correlation is evident between linoleic acid and fat deposition, surpassing that of palmitic acid and oleic acid, which have a higher relative content [11]. Realini et al. [49] investigated the relationship between IMF deposition and fatty acid composition in New Zealand sheep, yielding results consistent with our study, revealing a negative correlation between MUFA and IMF deposition, a positive correlation between PUFA and IMF deposition, and a correlation coefficient of -0.72 between linoleic acid and IMF deposition. This phenomenon might be attributed to the endogenous synthesis rate and desaturation sequence of SFA. Consequently, the distinctive fatty acid characteristics found in Ningxiang pork not only cater to the health requirements of consumers but also provide high-quality pork products.

4.2. Candidate genes for fatty acid composition

Currently, the molecular mechanisms underlying fat deposition continue to be a worthy subject. Fat deposition not only directly impacts the growth, development, and meat production traits of animals but also holds valuable implications for addressing human diseases. Ningxiang pigs, as an excellent model for obesity research, so more and more genes, regulatory factors, and metabolic pathways related to fat deposition in Ningxiang pigs have been identified [50–52]. In this study, we performed a comprehensive GWAS focusing on 14 fatty acids in the longissimus dorsi of Ningxiang pigs, and a majority of them exhibiting significant correlations with IMF content.

A total of 40 genes were identified from 37 significant loci associated with Saturated fat, which included hnRNPU [53,54], CEPT1 [55], ATP1B1 [56], DPT [57], DKK1 [58,59], PRKG1 [60–63], EXT2 [64], MEF2C [65,66], IL17RA [67], ITGA1 [68,69] and ALOX5 [70]. Among these, heteronuclear Heterogeneous ribonucleoprotein particles (hnRNPs) represent a group of proteins with diverse functions, playing pivotal roles in RNA biogenesis, cellular localization, and transport [71–73]. Specifically, heteronuclear Heterogeneous ribonucleoprotein particle U (hnRNP U) is involved in the Blnc1/hnRNPU/EBF2 Heterogeneous ribonucleoprotein particle complex, thus promoting the expression of brown adipocyte genes [53]. Additionally, Dickkopf WNT signaling pathway inhibitor 1 (DKK1) can regulate placental lipid metabolism through the WNT signaling pathway [58], as well as through ERK-PPAR γ- The CD36 axis enhances the ability of liver cells to uptake fatty acids [59]. Moreover, Extracellular glycosyltransferase 2 (EXT2) appears to be closely associated with fatty acid binding protein 4 and participates in lipid metabolism activities [74]. Surprisingly, Muscle cell enhancer factor 2C (MEF2C) not only plays a crucial regulatory role in skeletal muscle cells but also exerts significant regulatory effects on adipose tissue deposition [65], brown fat development [75], and muscular atrophy obesity [76] For instance, in Meishan pigs, MEF2C has been found to form a

cascade with miR222/SCD5, thereby regulating fatty acid metabolism [66]. Research has demonstrated that the signal of extracellular matrix (ECM) deposition induced by a High-Fat Diet is transmitted to adipocytes through the upregulation of integrin subunit α1 (ITGA1) and integrin subunit α7 (ITGA7), leading to the activation of the FAK-JNK/ERK1/2 signaling pathway in cells, which ultimately promotes adipogenesis in white adipose tissue [68]. Coincidentally, Arachidonic acid 5-nenenebb lipoxygenase (ALOX5) and its partner Arachidonic acid 5-lipoxygenase activator protein (ALOX5AP) are genes near C20:0 and C16:1 index significant correlation sites, respectively. ALOX5 and ALOX5AP are both involved in the browning of white adipose tissue through lipotoxin A4 [77] Furthermore, after ALOX5 knockout, the ability of adipogenic differentiation in mice is significantly increased [70]. In Ossabaw pig epicardial adipose tissue, ALOX5 is positively correlated with n-3 PUFAs [78].

Twenty five genes were annotated in the upstream and downstream regions of 21 loci related to Monounsaturated fatty acid. Among them, genes such as ALOX5AP [77], MEDAG [70], ISL1 [79], RXRB [80], CRY1 [81], and CDKAL1 [82,83] have been found to be related to lipid synthesis and metabolism. Interestingly, MEDAG and ALOX5AP belong to two genes upstream and downstream of the MARC0099145 locus. Additionally, MEDAG is involved in fat metabolism, playing a crucial role in back fat deposition in most Western pig breeds [84]. The study identified Retinol-X receptor β, the RXRB gene, as a powerful candidate gene due to its influence on the lipogenic activity of retinoic acid (bioactive vitamin A9). In the liver, the activation of RXRB leads to increased expression of stearyl CoA desaturation (SCD) and CD36 fatty acid transferase [80]. RXRB shows a negative correlation with PUFA, which is basically consistent with the results of this study and that of Black Iberian pig [85]. The Cryptochrome gene 1 (CRY1) is a member of the Circadian clock gene family and plays a vital role in adipocyte biology. CRY1 is regulated by the classic Wnt/β-catenin signaling pathway, which influences fat differentiation [86], Moreover, CRY1 contains two different interaction regions that regulate its degradation to achieve diurnal blood glucose control [87], further affecting conditions such as obesity [81,88].

Nineteen genes were annotated in the upstream and downstream regions of 16 loci related to PUFAs. Genes such as NDUFA4L2 [89], SLC16A7 [90], OTUB1 [91], EIF4E [92], and ROBO2 [93] were found to be associated with lipid synthesis and metabolism. Mitochondrial complex related protein 2 (NDUFA4L2) regulates obesity in rats through the PPAR signaling pathway and energy metabolism pathway [89], but mitochondrial dysfunction can cause an increase in NDUFA4L2 expression, leading to lipid accumulation in renal cells [94]. In addition, Solute carrier family 16 member 7 (SLC16A7), a 16 member of the plasmid family, is a key candidate gene related to the content of TG in chicken muscle tissue. In the way of IMF deposition in chicken Muscle cell, SLC16A7 can induce de novo adipogenesis [90]. Surprisingly, ssc-mir-708 is associated with fatty acids here, but mir-708 is currently only reported in the regulation of cardiomyocyte proliferation [95]. Finally, the eukaryotic translation initiation factor 4E (EIF4E) enhances the translation of various messenger RNAs involved in lipid metabolism processing and storage pathways, leading to weight gain after a high-fat diet [92]. These genes may influence the fatty acid composition. The majority of Ningxiang pigs exhibit medium to high heritability of fatty acids, indicating that candidate genes are likely to impact the fatty acid composition in the longissimus dorsi. Therefore, the candidate genes related to fatty acids identified in this study can be considered for enhancing the fatty acid composition of imported or commercial pig meat, thereby improving the meat quality of commercial pigs.

5. Conclusions

This genome-wide association study identified 74 genome-wide level SNPs associated with 14 fatty acids in *longissimus dorsi*. Some of SNPs were located within or near to reported genes, but some were novel for fatty acid compositions. Totally, 22 genes such as *hnRNPU*, *ALOX5AP*, and *NDUFA4L2* can be used as candidate genes for fatty acid compositions in Ningxiang pigs. Our findings will be helpful to understanding the genetic basis of fatty acid compositions and providing new targets for further breeding of pigs.

Supplementary Materials: The following supporting information can be downloaded at: www.mdpi.com/xxx/s1, Table S1: Detailed information on 25 fatty acids present in IMF of the longissimus dorsi of Ningxiang pigs; Appendix Material: GO and KEGG enrichment analysis.

Author Contributions: Conceptualization, Q.Z., H.G. and Y.Y.; methodology, H.G. and K.X.; software, Q.Z., G.S. and X.D.; validation, H.G. and S.Y.; formal analysis, Q.Z., and F.Y.; investigation, Y.P., Y.C. and X.H.; resources, J.H., Y.Y. and K.X.; data curation, F.Y., Y.F., Q.W., S.Y. and Z.J.; writing—original draft preparation, Q.Z., H.G., S.Y. and F.Y.; writing—review and editing, J.H., Y.P, Y.Y. and K.X.. visualization, H.G. and S.Y.; supervision, Y.Y. and K.X.; project administration, Y.Y. and K.X.; funding acquisition, Y.Y. and K.X. All authors have read and agreed to the published version of the manuscript.

Funding: This research was funded by the Laboratory of Lingnan Modern Agriculture Project (NT2021005), the Strategic Priority Research Program of Chinese Academy of Sciences (Grant No. XDA24030204), the Special Funds for the Construction of Innovative Provinces in Hunan (Grant numbers 2021NK1009 and 2021NK1012); the Natural Science Foundation of Hunan Province Project (2023JJ20043 and 2020JJ5635).

Institutional Review Board Statement: The experimental protocol used in this study was reviewed and approved by the Animal Experimental Ethical Inspection of Laboratory Animal Centre, Hunan Agricultural University. All sample collection was conducted under a permit (No. 2020047) approved by the Attitude of the Animal Management and Ethics Committee.

Informed Consent Statement: Not applicable.

Data Availability Statement: Not applicable.

Conflicts of Interest: The authors declare no conflict of interest.

References

1. Ou, S.; Cai, Y.; Chen, F.; He, S.; Chen, J.; Yang, L.; Ouyang, F.; He, J. Comparative Study on Growth Performance, Carcass Traits, and Meat Quality Traits of Ningxiang Pig and Du Long Hybrid Pig. *Swine Production* **2017**, 65-69, doi:10.13257/j.cnki.21-1104/s.2017.05.021.
2. Yang, F. Comparative Study on Gene Migration Analysis and GBC Estimation Methods in Ningxiang Pig Population. Master, Hunan Agricultural University, 2021.
3. Zhu, B.; Gao, H.; Yang, F.; Li, Y.; Yang, Q.; Liao, Y.; Guo, H.; Xu, K.; Tang, Z.; Gao, N.; et al. Comparative Characterization of Volatile Compounds of Ningxiang Pig, Duroc and Their Crosses (Duroc × Ningxiang) by Using SPME-GC-MS. *Foods (Basel, Switzerland)* **2023**, *12*, 1059, doi:10.3390/foods12051059.
4. Song, Y.; Gao, H.; Zhang, Y.; Yu, L.; He, J.; Xu, K. Determination of Carcass and Meat Quality Traits of Ningxiang Pig and Duning Binary Hybrid Pig. *Chinese Journal of Animal Husbandry* **2021**, *57*, 68-72, doi:10.19556/j.0258-7033.20210112-03.
5. Grassi, S.; Benedetti, S.; Opizzio, M.; Nardo, E.D.; Buratti, S. Meat and Fish Freshness Assessment by a Portable and Simplified Electronic Nose System (Mastersense). *Sensors (Basel)* **2019**, *19*, doi:10.3390/s19143225.
6. Khan, M.I.; Jo, C.; Tariq, M.R. Meat flavor precursors and factors influencing flavor precursors--A systematic review. *Meat Sci* **2015**, *110*, 278-284, doi:10.1016/j.meatsci.2015.08.002.
7. Guo, Q.; Kong, X.; Hu, C.; Zhou, B.; Wang, C.; Shen, Q.W. Fatty Acid Content, Flavor Compounds, and Sensory Quality of Pork Loin as Affected by Dietary Supplementation with l-arginine and Glutamic Acid. *J Food Sci* **2019**, *84*, 3445-3453, doi:10.1111/1750-3841.14959.
8. Bleicher, J.; Ebner, E.E.; Bak, K.H. Formation and Analysis of Volatile and Odor Compounds in Meat-A Review. *Molecules* **2022**, *27*, doi:10.3390/molecules27196703.
9. Chen, D.; Wang, X.; Guo, Q.; Deng, H.; Luo, J.; Yi, K.; Sun, A.; Chen, K.; Shen, Q. Muscle Fatty Acids, Meat Flavor Compounds and Sensory Characteristics of Xiangxi Yellow Cattle in Comparison to Aberdeen Angus. *Animals : an open access journal from MDPI* **2022**, *12*, doi:10.3390/ani12091161.
10. Zhao, Y. The Effect and Mechanism of Shallot Essential Oil on the Metabolism of Meat Sheep Fat and the Composition of Volatile Flavors. Doctor, Inner Mongolia Agricultural University, 2022.
11. Zhang, Y.; Zhang, J.; Gong, H.; Cui, L.; Zhang, W.; Ma, J.; Chen, C.; Ai, H.; Xiao, S.; Huang, L.; et al. Genetic correlation of fatty acid composition with growth, carcass, fat deposition and meat quality traits based on GWAS data in six pig populations. *Meat Sci* **2019**, *150*, 47-55, doi:10.1016/j.meatsci.2018.12.008.
12. Westerling, D.; Hedrick, H. Fatty Acid Composition of Bovine Lipids as Influenced by Diet, Sex and Anatomical Location and Relationship to Sensory Characteristics. *J Anim Sci* **1978**, *48*, doi:10.2527/jas1979.4861343x.

13. Melton, S.; Amiri, M.; Davis, G.; Backus, W. Flavor and Chemical Characteristics of Ground Beef from Grass-, Forage-Grain- and Grain-Finished Steers. *J Anim Sci* **1981**, *55*, doi:10.2527/jas1982.55177x.
14. de Oliveira Otto, M.C.; Wu, J.H.; Baylin, A.; Vaidya, D.; Rich, S.S.; Tsai, M.Y.; Jacobs, D.R., Jr.; Mozaffarian, D. Circulating and dietary omega-3 and omega-6 polyunsaturated fatty acids and incidence of CVD in the Multi-Ethnic Study of Atherosclerosis. *J Am Heart Assoc* **2013**, *2*, e000506, doi:10.1161/jaha.113.000506.
15. Lands, B.; Bibus, D.; Stark, K.D. Dynamic interactions of n-3 and n-6 fatty acid nutrients. *Prostaglandins, leukotrienes, and essential fatty acids* **2018**, *136*, 15-21, doi:10.1016/j.plefa.2017.01.012.
16. Lands, B. Historical perspectives on the impact of n-3 and n-6 nutrients on health. *Progress in lipid research* **2014**, *55*, 17-29, doi:10.1016/j.plipres.2014.04.002.
17. Merino, J.; Guasch-Ferré, M.; Ellervik, C.; Dashti, H.; Sharp, S.; Wu, P.; Overvad, K.; Sarnowski, C.; Kuokkanen, M.; Lemaitre, R.; et al. Quality of dietary fat and genetic risk of type 2 diabetes: individual participant data meta-analysis. *BMJ (Clinical research ed.)* **2019**, *366*, l4292, doi:10.1136/bmj.l4292.
18. Bibus, D.; Lands, B. Balancing proportions of competing omega-3 and omega-6 highly unsaturated fatty acids (HUFA) in tissue lipids. *Prostaglandins, leukotrienes, and essential fatty acids* **2015**, *99*, 19-23, doi:10.1016/j.plefa.2015.04.005.
19. Ding, R.; Yang, M.; Quan, J.; Li, S.; Zhuang, Z.; Zhou, S.; Zheng, E.; Hong, L.; Li, Z.; Cai, G.; et al. Single-Locus and Multi-Locus Genome-Wide Association Studies for Intramuscular Fat in Duroc Pigs. *Frontiers in genetics* **2019**, *10*, 619, doi:10.3389/fgene.2019.00619.
20. Wang, Y.; Ning, C.; Wang, C.; Guo, J.; Wang, J.; Wu, Y. Genome-wide association study for intramuscular fat content in Chinese Lulai black pigs. *Asian-Australas J Anim Sci* **2019**, *32*, 607-613, doi:10.5713/ajas.18.0483.
21. Viterbo, V.S.; Lopez, B.I.M.; Kang, H.; Kim, H.; Song, C.W.; Seo, K.S. Genome wide association study of fatty acid composition in Duroc swine. *Asian-Australas J Anim Sci* **2018**, *31*, 1127-1133, doi:10.5713/ajas.17.0779.
22. Purcell, S.; Neale, B.; Todd-Brown, K.; Thomas, L.; Ferreira, M.A.; Bender, D.; Maller, J.; Sklar, P.; de Bakker, P.I.; Daly, M.J.; et al. PLINK: a tool set for whole-genome association and population-based linkage analyses. *American journal of human genetics* **2007**, *81*, 559-575, doi:10.1086/519795.
23. Wang, J.; Zhang, Z. GAPIT Version 3: Boosting Power and Accuracy for Genomic Association and Prediction. *Genomics, proteomics & bioinformatics* **2021**, *19*, 629-640, doi:10.1016/j.gpb.2021.08.005.
24. Pook, T.; Mayer, M.; Geibel, J.; Weigend, S.; Cavero, D.; Schoen, C.C.; Simianer, H. Improving Imputation Quality in BEAGLE for Crop and Livestock Data. *G3 (Bethesda)* **2020**, *10*, 177-188, doi:10.1534/g3.119.400798.
25. Teslovich, T.; Musunuru, K.; Smith, A.; Edmondson, A.; Stylianou, I.; Koseki, M.; Pirruccello, J.; Ripatti, S.; Chasman, D.; Willer, C.; et al. Biological, Clinical, and Population Relevance of 95 Loci for Blood Lipids. *Nature* **2010**, *466*, 707-713, doi:10.1038/nature09270.
26. Yin, L.; Zhang, H.; Tang, Z.; Yin, D.; Fu, Y.; Yuan, X.; Li, X.; Liu, X.-L.; Zhao, S. HIBLUP: an integration of statistical models on the BLUP framework for efficient genetic evaluation using big genomic data. *Nucleic Acids Research* **2023**, *51*, doi:10.1093/nar/gkad074.
27. Raudvere, U.; Kolberg, L.; Kuzmin, I.; Arak, T.; Adler, P.; Peterson, H.; Vilo, J. g:Profiler: a web server for functional enrichment analysis and conversions of gene lists (2019 update). *Nucleic acids research* **2019**, *47*, doi:10.1093/nar/gkz369.
28. Chang, C.C.; Chow, C.C.; Tellier, L.C.; Vattikuti, S.; Purcell, S.M.; Lee, J.J. Second-generation PLINK: rising to the challenge of larger and richer datasets. *Gigascience* **2015**, *4*, 7, doi:10.1186/s13742-015-0047-8.
29. Huang, M.; Liu, X.; Zhou, Y.; Summers, R.M.; Zhang, Z. BLINK: a package for the next level of genome-wide association studies with both individuals and markers in the millions. *Gigascience* **2019**, *8*, doi:10.1093/gigascience/giy154.
30. Crespo-Piazuelo, D.; Criado-Mesas, L.; Revilla, M.; Castello, A.; Noguera, J.L.; Fernandez, A.I.; Ballester, M.; Folch, J.M. Identification of strong candidate genes for backfat and intramuscular fatty acid composition in three crosses based on the Iberian pig. *Sci Rep* **2020**, *10*, 13962, doi:10.1038/s41598-020-70894-2.
31. Jiang, Q.; Li, C.; Yu, Y.; Xing, Y.; Xiao, D.; Zhang, B. Comparison of fatty acid profile of three adipose tissues in Ningxiang pigs. *Anim Nutr* **2018**, *4*, 256-259, doi:10.1016/j.aninu.2018.05.006.
32. Zhang, W.; Zhang, J.; Cui, L.; Ma, J.; Chen, C.; Ai, H.; Xie, X.; Li, L.; Xiao, S.; Huang, L.; et al. Genetic architecture of fatty acid composition in the longissimus dorsi muscle revealed by genome-wide association studies on diverse pig populations. *Genet Sel Evol* **2016**, *48*, 5, doi:10.1186/s12711-016-0184-2.

33. Popova, T.; Givko, N. Fatty acid profile of the backfat layers in four pig breeds. *Food Science and Applied Biotechnology* **2019**, *2*, 24, doi:10.30721/fsab2019.v2.i1.66.
34. Lee, J.B.; Kang, Y.J.; Kim, S.G.; Woo, J.H.; Shin, M.C.; Park, N.G.; Yang, B.C.; Han, S.H.; Han, K.M.; Lim, H.T.; et al. GWAS and Post-GWAS High-Resolution Mapping Analyses Identify Strong Novel Candidate Genes Influencing the Fatty Acid Composition of the Longissimus dorsi Muscle in Pigs. *Genes* **2021**, *12*, doi:10.3390/genes12091323.
35. Xing, Y.; Wu, X.; Xie, C.; Xiao, D.; Zhang, B. Meat Quality and Fatty Acid Profiles of Chinese Ningxiang Pigs Following Supplementation with N-Carbamylglutamate. *Animals : an open access journal from MDPI* **2020**, *10*, doi:10.3390/ani10010088.
36. Xing, Y.; Yu, Y.; Xie, C.; Wu, X.; Xiao, D.; Yang, Z.; Zhang, B. Effect of Linseed Oil on Long Chain Fatty Acid Profile of Different Tissues in Ningxiang Pigs. *Chinese Journal of Animal Nutrition* **2020**, *32*, 2567-2574, doi:10.3969/j.issn.1006-267x.2020.06.016.
37. Zhu, B.; Niu, H.; Zhang, W.; Wang, Z.; Liang, Y.; Guan, L.; Guo, P.; Chen, Y.; Zhang, L.; Guo, Y.; et al. Genome wide association study and genomic prediction for fatty acid composition in Chinese Simmental beef cattle using high density SNP array. *BMC Genomics* **2017**, *18*, 464, doi:10.1186/s12864-017-3847-7.
38. Yang, B.; Zhang, W.; Zhang, Z.; Fan, Y.; Xie, X.; Ai, H.; Ma, J.; Xiao, S.; Huang, L.; Ren, J. Genome-wide association analyses for fatty acid composition in porcine muscle and abdominal fat tissues. *PloS one* **2013**, *8*, e65554, doi:10.1371/journal.pone.0065554.
39. Demets, R.; Gheysen, L.; Van Loey, A.; Foubert, I. Antioxidative capacity of microalgal carotenoids for stabilizing n-3LC-PUFA rich oil: Initial quantity is key. *Food Chem* **2023**, *406*, 135044, doi:10.1016/j.foodchem.2022.135044.
40. Wang, L.; Nong, Q.; Zhou, Y.; Sun, Y.; Chen, W.; Xie, J.; Zhu, X.; Shan, T. Changes in Serum Fatty Acid Composition and Metabolome-Microbiome Responses of Heigai Pigs Induced by Dietary N-6/n-3 Polyunsaturated Fatty Acid Ratio. *Front Microbiol* **2022**, *13*, 917558, doi:10.3389/fmicb.2022.917558.
41. Wang, L.; Zhang, S.; Huang, Y.; You, W.; Zhou, Y.; Chen, W.; Sun, Y.; Yi, W.; Sun, H.; Xie, J.; et al. CLA improves the lipo-nutritional quality of pork and regulates the gut microbiota in Heigai pigs. *Food Funct* **2022**, *13*, 12093-12104, doi:10.1039/d2fo02549c.
42. Mayer, C.; Côme, M.; Ulmann, L.; Martin, I.; Zittelli, G.C.; Faraloni, C.; Ouguerram, K.; Chénais, B.; Mimouni, V. The Potential of the Marine Microalga Diacronema lutheri in the Prevention of Obesity and Metabolic Syndrome in High-Fat-Fed Wistar Rats. *Molecules* **2022**, *27*, doi:10.3390/molecules27134246.
43. Calder, P.C. Very long-chain n-3 fatty acids and human health: fact, fiction and the future. *Proceedings of the Nutrition Society* **2018**, *77*, 52-72, doi:10.1017/S0029665117003950.
44. Nong, Q.; Wang, L.; Zhou, Y.; Sun, Y.; Chen, W.; Xie, J.; Zhu, X.; Shan, T. Low Dietary n-6/n-3 PUFA Ratio Regulates Meat Quality, Reduces Triglyceride Content, and Improves Fatty Acid Composition of Meat in Heigai Pigs. *Animals : an open access journal from MDPI* **2020**, *10*, doi:10.3390/ani10091543.
45. Waszkiewicz-Robak, B.; Szterk, A.; Rogalski, M.; Rambuszek, M.; Kruk, M.; Rokowska, E. Nutritional value of raw pork depending on the fat type contents in pigs feed. *Acta Sci Pol Technol Aliment* **2015**, *14*, 153-163, doi:10.17306/j.Afs.2015.2.17.
46. Xie, L.; Qin, J.; Rao, L.; Tang, X.; Cui, D.; Chen, L.; Xu, W.; Xiao, S.; Zhang, Z.; Huang, L. Accurate prediction and genome-wide association analysis of digital intramuscular fat content in longissimus muscle of pigs. *Anim Genet* **2021**, *52*, 633-644, doi:10.1111/age.13121.
47. Zhang, J.; Zhang, Y.; Gong, H.; Cui, L.; Huang, T.; Ai, H.; Ren, J.; Huang, L.; Yang, B. Genetic mapping using 1.4M SNP array refined loci for fatty acid composition traits in Chinese Erhualian and Bamaxiang pigs. *J Anim Breed Genet* **2017**, *134*, 472-483, doi:10.1111/jbg.12297.
48. Zhang, Z.; Zhang, Z.; Oyelami, F.O.; Sun, H.; Xu, Z.; Ma, P.; Wang, Q.; Pan, Y. Identification of genes related to intramuscular fat independent of backfat thickness in Duroc pigs using single-step genome-wide association. *Anim Genet* **2021**, *52*, 108-113, doi:10.1111/age.13012.
49. Gol, S.; Pena, R.N.; Rothschild, M.F.; Tor, M.; Estany, J. A polymorphism in the fatty acid desaturase-2 gene is associated with the arachidonic acid metabolism in pigs. *Sci Rep* **2018**, *8*, 14336, doi:10.1038/s41598-018-32710-w.
50. Criado-Mesas, L.; Ballester, M.; Crespo-Piazuelo, D.; Castello, A.; Benitez, R.; Fernandez, A.I.; Folch, J.M. Analysis of porcine IGF2 gene expression in adipose tissue and its effect on fatty acid composition. *PloS one* **2019**, *14*, e0220708, doi:10.1371/journal.pone.0220708.

51. Realini, C.E.; Pavan, E.; Purchas, R.W.; Agnew, M.; Johnson, P.L.; Bermingham, E.N.; Moon, C.D. Relationships between intramuscular fat percentage and fatty acid composition in M. longissimus lumborum of pasture-finished lambs in New Zealand. *Meat Sci* **2021**, *181*, 108618, doi:10.1016/j.meatsci.2021.108618.
52. Li, B.; Yang, J.; He, J.; Gong, Y.; Xiao, Y.; Zeng, Q.; Xu, K.; Duan, Y.; He, J.; Ma, H. Spatiotemporal Regulation and Functional Analysis of Circular RNAs in Skeletal Muscle and Subcutaneous Fat during Pig Growth. *Biology* **2021**, *10*, doi:10.3390/biology10090841.
53. Mi, L.; Zhao, X.Y.; Li, S.; Yang, G.; Lin, J.D. Conserved function of the long noncoding RNA Blnc1 in brown adipocyte differentiation. *Molecular metabolism* **2017**, *6*, 101-110, doi:10.1016/j.molmet.2016.10.010.
54. Shen, X.; Zhang, Y.; Ji, X.; Li, B.; Wang, Y.; Huang, Y.; Zhang, X.; Yu, J.; Zou, R.; Qin, D.; et al. Long Noncoding RNA lncRHL Regulates Hepatic VLDL Secretion by Modulating hnRNPU/BMAL1/MTTP Axis. *Diabetes* **2022**, *71*, 1915-1928, doi:10.2337/db21-1145.
55. Zayed, M.A.; Jin, X.; Yang, C.; Belaygorod, L.; Engel, C.; Desai, K.; Harroun, N.; Saffaf, O.; Patterson, B.W.; Hsu, F.F.; et al. CEPT1-Mediated Phospholipogenesis Regulates Endothelial Cell Function and Ischemia-Induced Angiogenesis Through PPARα. *Diabetes* **2021**, *70*, 549-561, doi:10.2337/db20-0635.
56. Lan, Q.; Liufu, S.; Liu, X.; Ai, N.; Xu, X.; Li, X.; Yu, Z.; Yin, Y.; Liu, M.; Ma, H. Comprehensive analysis of transcriptomic and metabolomic profiles uncovered the age-induced dynamic development pattern of subcutaneous fat in Ningxiang pig. *Gene* **2023**, *880*, 147624, doi:10.1016/j.gene.2023.147624.
57. Ningning, B. Research of Experssion of DPT and HTRA1 in Adipose tissue remodeling. Master, Shanghai Jiaotong University, 2018.
58. Strakovsky, R.S.; Pan, Y.X. A decrease in DKK1, a WNT inhibitor, contributes to placental lipid accumulation in an obesity-prone rat model. *Biology of reproduction* **2012**, *86*, 81, doi:10.1095/biolreprod.111.094482.
59. Yang, Z.; Huang, X.; Zhang, J.; You, K.; Xiong, Y.; Fang, J.; Getachew, A.; Cheng, Z.; Yu, X.; Wang, Y.; et al. Hepatic DKK1-driven steatosis is CD36 dependent. *Life science alliance* **2023**, *6*, doi:10.26508/lsa.202201665.
60. Zhang, W.; Li, X.; Jiang, Y.; Zhou, M.; Liu, L.; Su, S.; Xu, C.; Li, X.; Wang, C. Genetic architecture and selection of Anhui autochthonous pig population revealed by whole genome resequencing. *Frontiers in genetics* **2022**, *13*, 1022261, doi:10.3389/fgene.2022.1022261.
61. Li, C.; Sun, D.; Zhang, S.; Wang, S.; Wu, X.; Zhang, Q.; Liu, L.; Li, Y.; Qiao, L. Genome wide association study identifies 20 novel promising genes associated with milk fatty acid traits in Chinese Holstein. *PloS one* **2014**, *9*, e96186, doi:10.1371/journal.pone.0096186.
62. Revilla, M.; Puig-Oliveras, A.; Castelló, A.; Crespo-Piazuelo, D.; Paludo, E.; Fernández, A.I.; Ballester, M.; Folch, J.M. A global analysis of CNVs in swine using whole genome sequence data and association analysis with fatty acid composition and growth traits. *PloS one* **2017**, *12*, e0177014, doi:10.1371/journal.pone.0177014.
63. Shi, L.; Lv, X.; Liu, L.; Yang, Y.; Ma, Z.; Han, B.; Sun, D. A post-GWAS confirming effects of PRKG1 gene on milk fatty acids in a Chinese Holstein dairy population. *BMC Genet* **2019**, *20*, 53, doi:10.1186/s12863-019-0755-7.
64. Pedrosa, V.B.; Schenkel, F.S.; Chen, S.Y.; Oliveira, H.R.; Casey, T.M.; Melka, M.G.; Brito, L.F. Genomewide Association Analyses of Lactation Persistency and Milk Production Traits in Holstein Cattle Based on Imputed Whole-Genome Sequence Data. *Genes* **2021**, *12*, doi:10.3390/genes12111830.
65. Xu, Z.; Wu, J.; Zhou, J.; Zhang, Y.; Qiao, M.; Sun, H.; Li, Z.; Li, L.; Chen, N.; Oyelami, F.O.; et al. Integration of ATAC-seq and RNA-seq analysis identifies key genes affecting intramuscular fat content in pigs. *Frontiers in nutrition* **2022**, *9*, 1016956, doi:10.3389/fnut.2022.1016956.
66. Ren, H.; Xiao, W.; Qin, X.; Cai, G.; Chen, H.; Hua, Z.; Cheng, C.; Li, X.; Hua, W.; Xiao, H.; et al. Myostatin regulates fatty acid desaturation and fat deposition through MEF2C/miR222/SCD5 cascade in pigs. *Communications biology* **2020**, *3*, 612, doi:10.1038/s42003-020-01348-8.
67. Shinjo, T.; Iwashita, M.; Yamashita, A.; Sano, T.; Tsuruta, M.; Matsunaga, H.; Sanui, T.; Asano, T.; Nishimura, F. IL-17A synergistically enhances TNFα-induced IL-6 and CCL20 production in 3T3-L1 adipocytes. *Biochemical and biophysical research communications* **2016**, *477*, 241-246, doi:10.1016/j.bbrc.2016.06.049.
68. Chen, H.J.; Yan, X.Y.; Sun, A.; Zhang, L.; Zhang, J.; Yan, Y.E. High-Fat-Diet-Induced Extracellular Matrix Deposition Regulates Integrin-FAK Signals in Adipose Tissue to Promote Obesity. *Molecular nutrition & food research* **2022**, *66*, e2101088, doi:10.1002/mnfr.202101088.

69. Williams, A.S.; Kang, L.; Zheng, J.; Grueter, C.; Bracy, D.P.; James, F.D.; Pozzi, A.; Wasserman, D.H. Integrin α1-null mice exhibit improved fatty liver when fed a high fat diet despite severe hepatic insulin resistance. *The Journal of biological chemistry* **2015**, *290*, 6546-6557, doi:10.1074/jbc.M114.615716.
70. 70. Wu, Y.; Sun, H.; Song, F.; Huang, C.; Wang, J. Deletion of Alox5 gene decreases osteogenic differentiation but increases adipogenic differentiation of mouse induced pluripotent stem cells. *Cell and tissue research* **2014**, *358*, 135-147, doi:10.1007/s00441-014-1920-y.
71. Zhang, Z.; Feng, A.C.; Salisbury, D.; Liu, X.; Wu, X.; Kim, J.; Lapina, I.; Wang, D.; Lee, B.; Fraga, J.; et al. Collaborative interactions of heterogenous ribonucleoproteins contribute to transcriptional regulation of sterol metabolism in mice. *Nature communications* **2020**, *11*, 984, doi:10.1038/s41467-020-14711-4.
72. Zhao, M.; Shen, L.; Ouyang, Z.; Li, M.; Deng, G.; Yang, C.; Zheng, W.; Kong, L.; Wu, X.; Wu, X.; et al. Loss of hnRNP A1 in murine skeletal muscle exacerbates high-fat diet-induced onset of insulin resistance and hepatic steatosis. *Journal of molecular cell biology* **2020**, *12*, 277-290, doi:10.1093/jmcb/mjz050.
73. Hitachi, K.; Kiyofuji, Y.; Nakatani, M.; Tsuchida, K. Myoparr-Associated and -Independent Multiple Roles of Heterogeneous Nuclear Ribonucleoprotein K during Skeletal Muscle Cell Differentiation. *International journal of molecular sciences* **2021**, *23*, doi:10.3390/ijms23010108.
74. Bag, S.; Ramaiah, S.; Anbarasu, A. fabp4 is central to eight obesity associated genes: a functional gene network-based polymorphic study. *Journal of theoretical biology* **2015**, *364*, 344-354, doi:10.1016/j.jtbi.2014.09.034.
75. Wang, S.; Cao, Q.; Cui, X.; Jing, J.; Li, F.; Shi, H.; Xue, B.; Shi, H. Dnmt3b Deficiency in Myf5(+)-Brown Fat Precursor Cells Promotes Obesity in Female Mice. *Biomolecules* **2021**, *11*, doi:10.3390/biom11081087.
76. Sun, Q.Q.; Zhu, H.; Tang, H.Y.; Liu, Y.Y.; Chen, Y.Y.; Wang, S.; Qin, Y.; Gan, H.T.; Wang, S. RNA analysis of diet-induced sarcopenic obesity in rats. *Archives of gerontology and geriatrics* **2023**, *108*, 104920, doi:10.1016/j.archger.2022.104920.
77. Elias, I.; Ferré, T.; Vilà, L.; Muñoz, S.; Casellas, A.; Garcia, M.; Molas, M.; Agudo, J.; Roca, C.; Ruberte, J.; et al. ALOX5AP Overexpression in Adipose Tissue Leads to LXA4 Production and Protection Against Diet-Induced Obesity and Insulin Resistance. *Diabetes* **2016**, *65*, 2139-2150, doi:10.2337/db16-0040.
78. Walker, M.E.; Matthan, N.R.; Goldbaum, A.; Meng, H.; Lamon-Fava, S.; Lakshman, S.; Jang, S.; Molokin, A.; Solano-Aguilar, G.; Urban, J.F., Jr.; et al. Dietary patterns influence epicardial adipose tissue fatty acid composition and inflammatory gene expression in the Ossabaw pig. *The Journal of nutritional biochemistry* **2019**, *70*, 138-146, doi:10.1016/j.jnutbio.2019.04.013.
79. Li, H.; Heilbronn, L.K.; Hu, D.; Poynten, A.M.; Blackburn, M.A.; Shirkhedkar, D.P.; Kaplan, W.H.; Kriketos, A.D.; Ye, J.; Chisholm, D.J. Islet-1: a potentially important role for an islet cell gene in visceral fat. *Obesity (Silver Spring, Md.)* **2008**, *16*, 356-362, doi:10.1038/oby.2007.76.
80. Singh Ahuja, H.; Liu, S.; Crombie, D.L.; Boehm, M.; Leibowitz, M.D.; Heyman, R.A.; Depre, C.; Nagy, L.; Tontonoz, P.; Davies, P.J. Differential effects of rexinoids and thiazolidinediones on metabolic gene expression in diabetic rodents. *Molecular pharmacology* **2001**, *59*, 765-773, doi:10.1124/mol.59.4.765.
81. Griebel, G.; Ravinet-Trillou, C.; Beeské, S.; Avenet, P.; Pichat, P. Mice deficient in cryptochrome 1 (cry1 (-/-)) exhibit resistance to obesity induced by a high-fat diet. *Frontiers in endocrinology* **2014**, *5*, 49, doi:10.3389/fendo.2014.00049.
82. Choi, W.J.; Jin, H.S.; Kim, S.S.; Shin, D. Dietary Protein and Fat Intake Affects Diabetes Risk with CDKAL1 Genetic Variants in Korean Adults. *International journal of molecular sciences* **2020**, *21*, doi:10.3390/ijms21165607.
83. Zhu, J.; Xu, D.; Yang, R.; Liu, M.; Liu, Y. The triglyceride glucose index and CDKAL1 gene rs10946398 SNP are associated with NAFLD in Chinese adults. *Minerva endocrinology* **2023**, *48*, 51-58, doi:10.23736/s2724-6507.20.03273-3.
84. Gozalo-Marcilla, M.; Buntjer, J.; Johnsson, M.; Batista, L.; Diez, F.; Werner, C.R.; Chen, C.Y.; Gorjanc, G.; Mellanby, R.J.; Hickey, J.M.; et al. Genetic architecture and major genes for backfat thickness in pig lines of diverse genetic backgrounds. *Genet Sel Evol* **2021**, *53*, 76, doi:10.1186/s12711-021-00671-w.
85. Pena, R.N.; Noguera, J.L.; García-Santana, M.J.; González, E.; Tejeda, J.F.; Ros-Freixedes, R.; Ibáñez-Escriche, N. Five genomic regions have a major impact on fat composition in Iberian pigs. *Sci Rep* **2019**, *9*, 2031, doi:10.1038/s41598-019-38622-7.
86. Sun, S.; Zhou, L.; Yu, Y.; Zhang, T.; Wang, M. Knocking down clock control gene CRY1 decreases adipogenesis via canonical Wnt/β-catenin signaling pathway. *Biochemical and biophysical research communications* **2018**, *506*, 746-753, doi:10.1016/j.bbrc.2018.10.134.

87. Toledo, M.; Batista-Gonzalez, A.; Merheb, E.; Aoun, M.L.; Tarabra, E.; Feng, D.; Sarparanta, J.; Merlo, P.; Botrè, F.; Schwartz, G.J.; et al. Autophagy Regulates the Liver Clock and Glucose Metabolism by Degrading CRY1. *Cell metabolism* **2018**, *28*, 268-281.e264, doi:10.1016/j.cmet.2018.05.023.
88. Sardon Puig, L.; Pillon, N.J.; Näslund, E.; Krook, A.; Zierath, J.R. Influence of obesity, weight loss, and free fatty acids on skeletal muscle clock gene expression. *American journal of physiology. Endocrinology and metabolism* **2020**, *318*, E1-e10, doi:10.1152/ajpendo.00289.2019.
89. Wei, H.; Lin, X.; Liu, L.; Peng, X. Flaxseed Polysaccharide Alters Colonic Gene Expression of Lipid Metabolism and Energy Metabolism in Obese Rats. *Foods (Basel, Switzerland)* **2022**, *11*, doi:10.3390/foods11131991.
90. Wang, Y.; Liu, L.; Liu, X.; Tan, X.; Zhu, Y.; Luo, N.; Zhao, G.; Cui, H.; Wen, J. SLC16A7 Promotes Triglyceride Deposition by De Novo Lipogenesis in Chicken Muscle Tissue. *Biology* **2022**, *11*, doi:10.3390/biology11111547.
91. Zhang, J.L.; Du, B.B.; Zhang, D.H.; Li, H.; Kong, L.Y.; Fan, G.J.; Li, Y.P.; Li, P.C.; Liang, C.; Wang, Z.; et al. OTUB1 alleviates NASH through inhibition of the TRAF6-ASK1 signaling pathways. *Hepatology (Baltimore, Md.)* **2022**, *75*, 1218-1234, doi:10.1002/hep.32179.
92. Conn, C.S.; Yang, H.; Tom, H.J.; Ikeda, K.; Oses-Prieto, J.A.; Vu, H.; Oguri, Y.; Nair, S.; Gill, R.M.; Kajimura, S.; et al. The major cap-binding protein eIF4E regulates lipid homeostasis and diet-induced obesity. *Nature metabolism* **2021**, *3*, 244-257, doi:10.1038/s42255-021-00349-z.
93. Mohammadi, H.; Farahani, A.H.K.; Moradi, M.H.; Mastrangelo, S.; Di Gerlando, R.; Sardina, M.T.; Scatassa, M.L.; Portolano, B.; Tolone, M. Weighted Single-Step Genome-Wide Association Study Uncovers Known and Novel Candidate Genomic Regions for Milk Production Traits and Somatic Cell Score in Valle del Belice Dairy Sheep. *Animals : an open access journal from MDPI* **2022**, *12*, doi:10.3390/ani12091155.
94. Laursen, K.B.; Chen, Q.; Khani, F.; Attarwala, N.; Gross, S.S.; Dow, L.; Nanus, D.M.; Gudas, L.J. Mitochondrial Ndufa4l2 Enhances Deposition of Lipids and Expression of Ca9 in the TRACK Model of Early Clear Cell Renal Cell Carcinoma. *Frontiers in oncology* **2021**, *11*, 783856, doi:10.3389/fonc.2021.783856.
95. Deng, S.; Zhao, Q.; Zhen, L.; Zhang, C.; Liu, C.; Wang, G.; Zhang, L.; Bao, L.; Lu, Y.; Meng, L.; et al. Neonatal Heart-Enriched miR-708 Promotes Proliferation and Stress Resistance of Cardiomyocytes in Rodents. *Theranostics* **2017**, *7*, 1953-1965, doi:10.7150/thno.16478.